J Mater Sci (2012) 47:4845–4850
DOI 10.1007/s10853-012-6345-y

α'-Martensite formation in deep-drawn Mn-based TWIP steel

R. T. van Tol · J. K. Kim · L. Zhao · J. Sietsma · B. C. De Cooman

Received: 19 December 2011 / Accepted: 13 February 2012 / Published online: 17 March 2012

Abstract To understand the formation of α'-martensite in high stacking fault energy twinning-induced plasticity steel deformed in the deep drawing mode, the existing phases were investigated using magnetic and transmission electron microscopy (TEM). Small fractions of α'-martensite were quantitatively determined by magnetization saturation experiments and further observed by TEM. TEM revealed the formation of α'-martensite at shear band and twin intersections.

Introduction

In order to improve passenger safety and fuel economy, the use of advanced high strength steel (AHSS) in the automotive industry has increased significantly in the last decade, and TWinning-Induced Plasticity (TWIP) steels are the focus of research efforts aiming to develop them into an entirely new class of ultra-high strength automotive steel grades with a superior strain hardening behaviour. Austenitic Mn-based TWIP steels, which combine high strength with high ductility, have strain hardening properties resulting from deformation mechanisms involving twinning or plasticity-induced transformation [1–6]. The occurrence of these plasticity-enhancing mechanisms is related to the austenite phase (γ) stability. Austenite with a relatively low stability can transform to α'-martensite by means of the γ (FCC) $\rightarrow$ ε (HCP) $\rightarrow$ α' (BCC) sequence of martensitic transformations. Suppression of the strain-induced $\gamma \rightarrow \varepsilon$ martensite transformation is therefore considered to imply stability against α'-martensite formation [7]. It has been argued on the basis of thermodynamic considerations [8–10] that Mn-based TWIP steel with a stacking fault energy (SFE) higher than approximately 18 mJ/m^2 will not undergo strain-induced ε-martensite formation. According to Olson and Cohen [11, 12], however, a low SFE promotes strain-induced nucleation of α'-martensite, which does not necessarily require the intermediate formation of ε-martensite. They and other authors [13–17] also suggested the possibility of a direct α'-martensite formation from austenite without the intermediate transformation to ε-martensite. The material examined in the present contribution did not show any evidence of α'-martensite formation when tested in a conventional uni-axial test [17]. Direct experimental evidence for the $\gamma \rightarrow \alpha'$-martensite transformation has not yet been reported for Mn-based steel [18]. The aim of the present work is, therefore, to investigate the formation of α'-martensite from austenite in a deep-drawn austenitic Mn-based TWIP steel with high SFE using both magnetic and transmission electron microscopy (TEM) techniques.

Experimental

The examined material was a 1.7-mm thick 0.7% C–15% Mn–3% Al TWIP steel (in wt%) with a fully austenitic

R. T. van Tol (✉)
Tata Steel Research Development & Technology,
Wenckebachstraat 1, 1970 CA IJmuiden, The Netherlands
e-mail: ron.van-tol@tatasteel.com

R. T. van Tol · L. Zhao
Materials Innovation Institute, Mekelweg 2, 2628 CD Delft, The Netherlands

R. T. van Tol · L. Zhao · J. Sietsma
Department of Materials Science and Engineering, Delft University of Technology, Mekelweg 2, 2628 CD Delft, The Netherlands

J. K. Kim · B. C. De Cooman
Pohang University of Science and Technology,
Graduate Institute of Ferrous Technology, San 31,
Pohang 790-784, South Korea

microstructure at room temperature. The precise chemical composition of the steel is listed in Table 1. Taking into account the effect of the Si and Al additions on the SFE by means of literature data (-7 mJ/m^2 per wt% Si and $+10$ mJ/m^2 per wt% Al), the SFE was calculated to be $5 \times 10^1 \pm 1 \times 10^1$ mJ/m^2 [8, 19, 20]. The properties of the TWIP steel were measured in the cold rolled and recrystallization-annealed condition. Table 1 also lists the mechanical properties. The sheets were cut into round blanks with a diameter of 102.5 mm by water jet cutting to avoid deformation and heating of the cut edge during sample preparation. The blanks were subsequently formed into cups by deep drawing on an Erichsen press with a ratio of blank diameter to punch diameter of 2.05. Table 2 lists the deep drawing parameters.

The α'-martensite fraction was determined by magnetic measurements to verify the effect of the accumulated equivalent strain and the angle to the rolling direction. For the magnetization experiments samples with a size of approximately 2 mm $\times$ 2 mm $\times$ t, where t is the local sample thickness [16], were machined from the deep drawn cups by spark erosion. The samples were taken along the cup wall in the direction which was originally transverse to the sheet rolling direction and along the circumference of the cup at 35 mm from the cup bottom (Fig. 1). At 35 mm from the cup bottom in the direction transverse to the rolling direction, a sample was cut into two pieces by spark erosion: one sample was taken from the inner side of the cup, another sample was taken from the outer side of the cup. All magnetic measurements were performed using a Lake Shore 7307 Vibrating Sample Magnetometer (VSM). Before the experiments the VSM was calibrated with a standard NIST nickel specimen. The samples were magnetized in an external field from -1.5 to 1.5 T. This field strength is high enough to achieve magnetic saturation of the ferromagnetic phases [21]. The weight fraction of α'-martensite, the only ferromagnetic phase present in this otherwise paramagnetic material with phases such as austenite and ε-martensite (if any), was estimated by

$$f(\alpha') = \frac{M_s}{x_{Fe} M_{s,Fe}}, \quad (1)$$

where M_s is the magnetization of the α'-martensite, calculated from the measured magnetization of the sample minus the magnetic contribution of the austenite to determine the small fraction of α'-martensite in the present case. The item $M_{s,Fe}$ is the magnetization of pure iron at room temperature, which was determined in a separate measurement at 215 A m^2/kg and x_{Fe} represents the atomic fraction of Fe in the material.

TEM was carried out on a JEOL JEM-2100F transmission electron microscope operating at 200 kV to verify the presence of α'-martensite in the microstructure by electron diffraction. Focus ion beam (FIB) was performed on a FEI Company Quanta 3D FEG (Fig. 2) to prepare the TEM sample at the position with the highest accumulated equivalent strain, 35 mm from the cup bottom at the inner side of the deep-drawn cup in transverse direction (Fig. 3). The accumulated equivalent strain was determined by finite element method (FEM) simulations of the cup deep drawing process [17].

Results

Figure 1 shows the α'-martensite fraction as a function of the accumulated equivalent strain averaged over the sample's thickness measured by VSM. There is an initial α'-martensite fraction of approximately 0.2%. An equivalent strain of more than 0.5, results in the formation of strain-induced α'-martensite. At 35 mm from the cup bottom at the inner side of the cup the accumulated equivalent strain was approximately 0.85. The maximum volume fraction of 1.2% α'-martensite was measured at this position.

The inset in Fig. 1 shows the α'-martensite fraction as a function of the angle to the rolling direction. The measurements were made on the deep drawn cup at 35 mm from the cup bottom where the accumulated equivalent

Table 2 Deep-drawing parameters

Blank holder force (kN)	20–30
Punch speed (mm/s)	1.5
Punch diameter (mm)	50
Punch edge radius (mm)	7.5
Die diameter (mm)	54.8
Die edge radius (mm)	6.0
Lubrication	Teflon foil
Temperature (°C)	20

Table 1 Composition and mechanical properties of Mn-based TWIP steel

C (wt%)	Si (wt%)	Mn (wt%)	Al (wt%)	Yield strength $\sigma_{0.2}$ (MPa)	Ultimate tensile strength σ_{UTS} (MPa)	Elongation at ultimate tensile strength ε_{UTS} (%)	Elongation at fracture ε_f (%)
0.71	0.07	14.55	2.93	504	875	40.0	43.1

The mechanical properties are averaged over the rolling direction

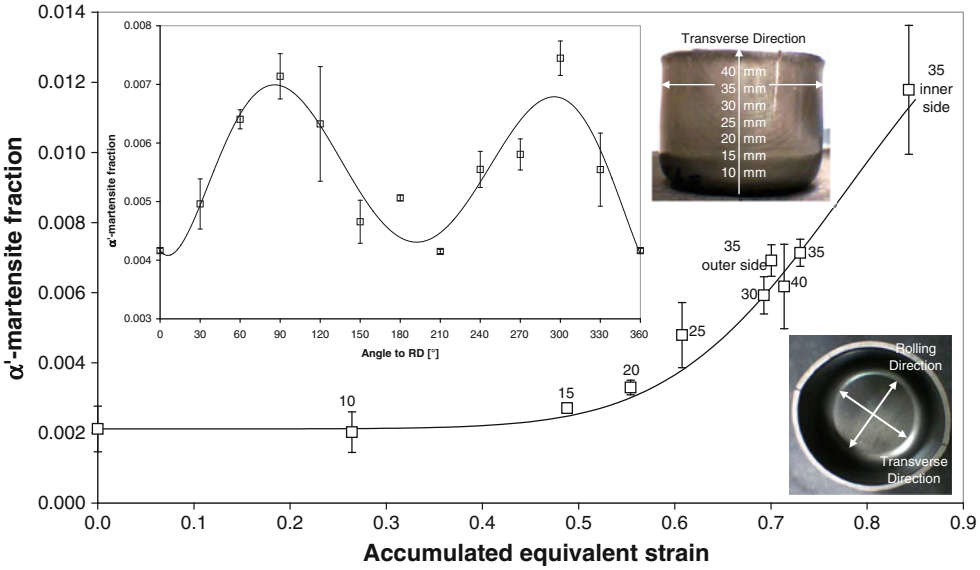

Fig. 1 α'-Martensite fraction, determined by magnetic saturation measurements on deep drawn cup walls, as a function of accumulated equivalent strain. The distance from the deep-drawn cup bottom is indicated in mm next to each data point. The labels '*inner side*' and '*outer side*' are for the measurements made on the inside and the outside of a cup wall sample taken 35 mm from the cup bottom in the direction transverse to the *rolling direction*. The *inset* shows the α'-martensite fraction in a deep drawn cup at a distance of 35 mm from the cup bottom as a function of the angle to the *rolling direction*

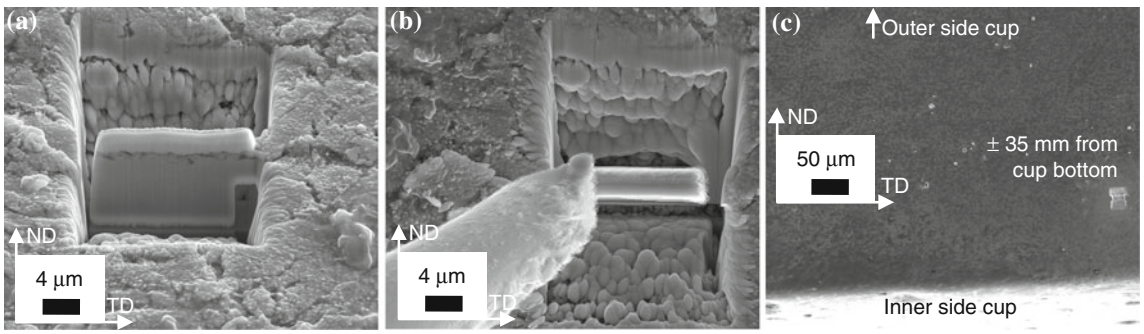

Fig. 2 FIB: **a** cutting and **b** removal of the TEM sample from the cross-section (**c**) at the *inner side* of the deep-drawn cup at 35 mm from the *cup bottom* in *transverse direction*

strain was about 0.73. The results indicate a systematic trend as a function of the angle to the rolling direction. The maximum α'-martensite fraction in the material can be found located in the transverse direction from the original centre of the blank, which most probably is related to the development of texture.

Figure 3 shows bright field (BF) images and related selected area diffraction patterns (SADP) from the TEM sample taken at 35 mm from the cup bottom on the inner side of a deep-drawn cup in transverse direction. The plasticity mechanisms were found to consist of a pronounced planar dislocation glide and the formation of planar features and bands related to the overlapping of multiple planar stacking faults, i.e. shear bands and narrow twins. The SADPs clearly indicate that not all narrow planar features in the highly deformed TWIP steel are twins. In fact, many band-type features are found to be shear bands rather than twins. None of the diffraction patterns indicates the presence of ε-martensite. Considering the SFE of the alloy, the absence of ε-martensite and the presence of shear bands is not unexpected. The orientation relationships between austenite and α'-martensite obey the Kurdjumov–Sachs orientation relationship between α'-martensite and austenite:

$$\begin{aligned} \{111\}_{\gamma} // \{110\}_{\alpha'} \\ \langle 110\rangle_{\gamma} // \langle 111\rangle_{\alpha'} \end{aligned} \quad (2)$$

The micrograph in Fig. 3a shows a highly dislocated microstructure containing one clear band. The SADP reveals the band to be a shear band, rather than a twin, and shows the presence of α'-martensite. A secondary shear band system is also present, indicated by dashed white

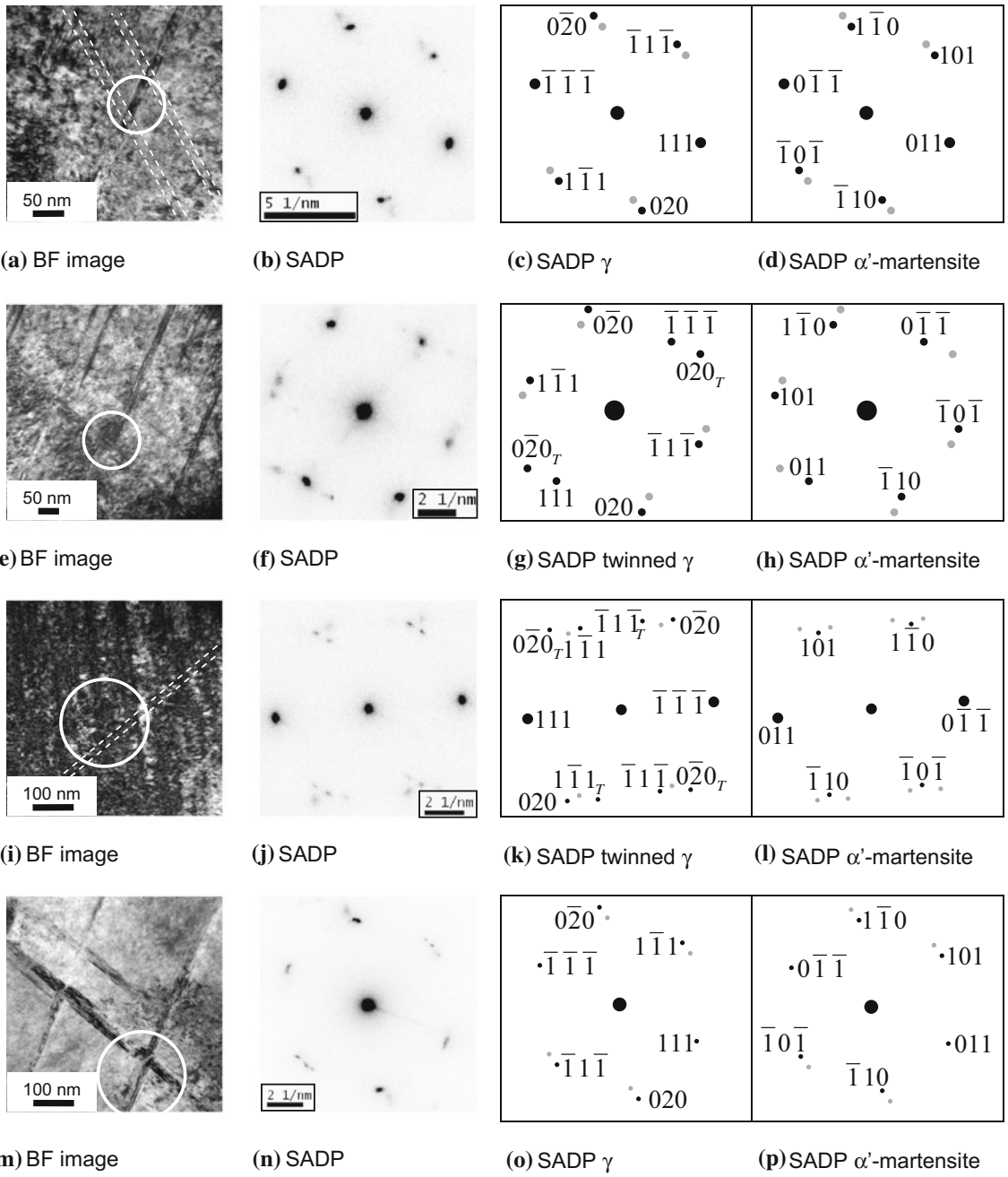

Fig. 3 α'-Martensite at intersection of **a–d** shear bands, **e–h** twin and shear band, **i–l** twins and **m–p** shear bands. The TEM sample was taken 35 mm from the cup bottom on the inner side of the deep-drawn cup. The *white circles* indicate the positions where the SADPs were taken. The *dashed white lines* in **a** and **i** indicate the position of shear bands with a low contrast. The *black diffraction spots* in the schematic SADPs in the *third column* are for the γ phase and include the relevant twin reflections. The *black diffraction spots* in the schematic SADPs in the *fourth column* are for the α'-martensite. The *grey spots* in the schematic SADPs indicate the diffraction spots of the other phase

lines. The BF image (Fig. 3e) and the corresponding SADP (Fig. 3f) are for the two shear band systems and their intersection. The microstructure is severely deformed and contains a high dislocation density. The diffraction pattern reveals the presence of α'-martensite at the intersection between twins and shear bands. The high defect concentration at this type of intersections makes them very effective nucleation sites for strain-induced transformation [8, 11, 12]. Figure 3i–n shows additional BF images and corresponding SADPs from the TEM sample. Owing to the intense deformation, the deformation bands have a low diffraction contrast and the dashed white lines indicate the position of parallel shear bands, which are not clearly visible. The diffraction pattern however clearly reveals the

presence of α'-martensite. The BF image in Fig. 3m shows two intersecting shear band systems, which are clearly visible despite the high dislocation density. The SADPs clearly reveal the presence of α'-martensite at shear band-shear band intersections.

Discussion

It has been reported that the deformation mechanisms responsible for the mechanical properties of austenitic Mn-based TWIP steels are related to the austenite stability and involve dislocation slip, twinning and deformation-induced transformation to martensite [1–6]. With increasing accumulated equivalent strain, deformation is facilitated initially by dislocation multiplication, followed by twinning and/or martensitic transformations, providing barriers for further dislocation slip [1–6].

Stability against the $\gamma \rightarrow \varepsilon$-martensite transformation is usually considered to imply stability against the $\gamma \rightarrow \alpha'$-martensite transformation [7], since ε-martensite laths form as an intermediate phase. The present magnetic measurements indicate strain-induced α'-martensite formation by revealing a small volume fraction of α'-martensite when the accumulated equivalent strain is 0.5 or higher. TEM foil preparation does not induce such high accumulated equivalent strains and will therefore not be the origin for α'-martensite formation. The formation of α'-martensite is a three-dimensional phenomenon, being observed by TEM through thin sections. The widely held view is that α'-martensite must have ε-martensite as a precursor [7]. In Mn-based TWIP steels, α'-martensite is known to form at the intersections of shear bands like slip bands, twins and/or ε-martensite laths [11, 12]. The sequential nature of the $\gamma \rightarrow \varepsilon \rightarrow \alpha'$ martensitic transformation at intersected ε-martensite laths and the increasing volume fraction of α'-martensite upon straining implies the simultaneous presence of ε- and α'-martensite. According to Olson and Cohen [11, 12], the sequential $\gamma \rightarrow \varepsilon \rightarrow \alpha'$ martensitic transformation requires the intersection of at least one ε-martensite lath, which was not observed (Fig. 3). ε-Martensite could only have been a precursor of α'-martensite formation in case of complete $\varepsilon \rightarrow \alpha'$-martensite transformation. Transformation from ε-martensite laths would have led to α'-martensite formation outside the intersected regions and higher α'-martensite fractions, which was not observed in the present work. The presence of ε-martensite as an intermediate phase at the intersected regions is untraceable after complete transformation to α'-martensite. We can conclude that the present observations question the $\gamma \rightarrow \varepsilon \rightarrow \alpha'$ martensitic transformation as described by Olson and Cohen [11, 12]. The results strongly indicate that strain-induced nucleation of α'-martensite does not necessarily require the intermediate formation of ε-martensite laths.

In Mn-based TWIP steels with low SFE, α'-martensite is known to form at the intersections of bands like shear bands, twins and/or ε-martensite laths [11, 12] as seen in Fig. 3e and m. These intersected bands can be very effective as nucleation sites, allowing the passage of previously blocked dislocations, inducing the formation of α'-martensite [11, 12] and releasing stress concentrations [8]. Also in the Fig. 3a and i, secondary band systems have been observed, although less clearly as in the Fig. 3e and m.

The results show that the formation of α'-martensite in the bulk material is related to both the accumulated equivalent strain and the crystallographic texture. One can assume the crystallographic texture components of the examined material to be a function of the angle to the rolling direction. The formation of α'-martensite in the material relates to the location of the material with respect to the rolling direction. This observation is indicative of a relation between the formation of α'-martensite and the development of crystallographic texture during deep drawing. Similar Mn-based TWIP steels do not show planar anisotropy [22], suggesting subtle texture effects leading to anisotropy in strain-induced martensite formation. The transverse direction to the rolling direction has apparently a more favourable crystallographic texture for α'-martensite formation than the rolling direction. Lo et al. [23] mentioned that twin-matrix lamellae, generated by heavy rolling deformation, are often oriented along the rolling direction. Slip along the $\{111\}$ planes in the rolling direction and twinning is gradually suppressed as deformation proceeds, but slip along the $\{111\}$ planes that are not parallel to the lamellae is activated. In the present work, deep drawn material shows a high accumulated strain. It is also known that tensile deformation of medium SFE FCC metals or alloys favours the formation of twins in grains oriented with a $\langle 111 \rangle$ direction parallel to the tensile axis. It is therefore possible that straining in the transverse direction can also activate the formation of strain induced martensitic transformation along the transverse direction.

Conclusion

In conclusion, magnetic and TEM techniques were used to investigate the formation of α'-martensite in an austenitic Mn-based TWIP steel. It is found that despite its high SFE (5×10^1 mJ/m^2), deep drawing deformation results in the formation of α'-martensite, which is attributed to the accumulated equivalent strain and crystallographic texture. The presence of α'-martensite at shear band and twin intersections is observed and question the sequential $\gamma \rightarrow \varepsilon \rightarrow \alpha'$ martensitic transformation. The present work indicates that the formation of α'-martensite in a high SFE

FCC alloy does not necessarily require the intermediate formation of ε-martensite laths.

Acknowledgements This research was carried out under the project number MC5.07292 in the framework of the Research Program of the Materials innovation institute (M2i) (www.m2i.nl). The support of M2i and Tata Steel is gratefully acknowledged. The authors wish to thank Menno de Bruine (Tata Steel) for his technical support in the deep drawing experiments. The authors also wish to thank Tae Jin Song and Lawrence Cho (GIFT-POSTECH) for performing TEM and focused ion beam, respectively, and Sjoerd van Dellen, Henrik van den Heuvel, Tjerk Koopmans and Vincent Serle (TU Delft) for the magnetic saturation measurements and the stimulating discussions.

References

1. Frommeyer G, Brüx U, Neumann P (2003) ISIJ Int 43(3):438
2. Scott C, Guelton N, Allain S, Faral M (2005) The development of a new Fe-Mn-C austenitic steel for automotive applications. In: Developments in sheet products for automotive applications. Materials science & technology 2005, pp 127–138
3. Efstathiou C, Sehitoglu H (2010) Acta Mater 58:1479
4. Barbier D, Gey N, Allain S, Bozzolo N, Humbert M (2009) Mater Sci Eng A 500:196
5. Liang X, McDermid JR, Bouaziz O, Wang X, Embury JD, Zurob HS (2009) Acta Mater 57:3978
6. Curtze S, Kuokkala V-T (2010) Acta Mater 58:5129
7. Bouaziz O, Allain S, Scott CP, Cugy P, Barbier D (2011) Curr Opin Solid State Mater Sci 15:141
8. Oh BW, Cho SJ, Kim YG, Kim WS, Hong SH (1995) Mater Sci Eng A 197:147
9. Bracke L (2007) Deformation behaviour of austenitic Fe–Mn alloys by twinning and martensitic transformation. PhD thesis, University of Ghent, Ghent
10. Allain S, Château J-P, Bouaziz O, Migot S, Guelton N (2004) Mater Sci Eng A 387–389:158
11. Olson GB, Cohen M (1972) J Less-Common Met 28:107
12. Olson GB, Cohen M (1975) Metall Trans 6A:791
13. Huang BX, Wang XD, Rong YH, Wang L, Jin L (2006) Mater Sci Eng A 438–440:306
14. Ding H, Ding H, Song D, Tang S, Yang P (2011) Mater Sci Eng A 528:868
15. Sato K, Ichinose M, Hirotsu Y, Inoue Y (1989) ISIJ Int 29:868
16. van Tol RT, Zhao L, Schut H, Sietsma J (2012) Mater Sci Technol 28(3):348
17. van Tol RT, Zhao L, Sietsma J (2011) The 1st international conference on high Mn TWIP steels HMnS2011, May 2011, Seoul
18. Tomota Y, Strum M, Morris JW (1986) Metall Trans 17A:537
19. Bleck W, Phiu-on K, Heering C, Hirt G (2007) Steel Res Int 78(7):536
20. Gallagher PCJ (1970) Metall Trans 1:2429
21. Zhao L, van Dijk NH, Brück E, Sietsma J, van der Zwaag S (2001) Mater Sci Eng A 313:145
22. Xu L, Barlat F (2011) The 1st international conference on high Mn TWIP steels HMnS2011, May 2011, Seoul
23. Lo KH, Shek CH, Lai JKL (2009) Mater Sci Eng R 65:39